Electronic Supporting Information (ESI)

Direct photolysis and nitrite-sensitized indirect photolysis of effluent-derived phenolic contaminants under UV_{254} irradiation

Yueyue Li[a], Lixiao Wang[a], Haiyan Xu[a], Junhe Lu[a], Jean-Marc Chovelon[b], Yuefei Ji[a,*]

[a] *College of Resources and Environmental Sciences, Nanjing Agricultural University, Nanjing 210095, China*

[b] *Univ Lyon, Université Claude Bernard Lyon 1, CNRS, IRCELYON, F-69626, Villeurbanne, France*

[*] Corresponding author. Yuefei Ji, College of Resources and Environmental Sciences, Nanjing Agricultural University, Nanjing 210095, China.
E-mail addresses: yuefeiji@njau.edu.cn (Y. Ji).

Text S1. Reagents and materials

Bisphenol A (BPA, 99%), isopropanol (*i*-PrOH, ≥ 99.5%), and sodium nitrite ($NaNO_2$) were purchased from Sigma-Aldrich (St, Louis, MO, USA). Acetaminophen (ATP, 99%) was purchased from Macklin Company (Shanghai, China). 2,4-Dihydroxybenzophenone (BP1, ≥ 98%) was obtained from TCI Company (Tokyo, Japan). Salbutamol sulfate (SAL, 99%) was purchased from Yuanye Reagent Co. Ltd (Nanjing, China). Chromatographic acetonitrile (ACN), methanol (MeOH), and formic acid were obtained from Burdick & Jackson (Muskegon, MI, USA). All other reagents were of analytical purity or higher grade. Suwanee River natural organic matter (SRNOM, 2R101N) was purchased from the International Humus Society (St. Paul, MN, USA).

Text S2. Identification of intermediate products by LC-qTOF-MS/MS

The SPE-concentrated samples were analyzed by LC-qTOF-MS/MS to identify the phenolic compounds and their TPs. Analytical separation was achieved by a Kinetex LC-C_{18} reversed-phase column (2.6 μm, 100 mm × 2.1 mm, i.d.). The mobile phase was a mixture of 50% MeOH and 50% Milli-Q water at a flow rate of 0.3 mL min^{-1}, and the injection volume was 2 μL. Mass spectrometer worked under negative ion mode using an electrospray ionization source (ESI). Instrumental parameters were as follows: ion spray voltage (ISVF), 4500 V; ion source temperature (TEM), 550 ^{o}C; atomizing gas (GS1), 65 psi; auxiliary gas (GS2), 65 psi; curtain gas (CUR), 35 psi. The mass spectrum data acquisition mode was the full scanning of high-resolution time-of-flight mass spectrometry (TOF MS) and simultaneously triggered acquisition of high-resolution secondary mass spectrometry (TOF MS IDA MS/MS). The resolution of the mass spectrometry was 30000 (500 *m/z* FWHM). The scanning range of TOF-MS and IDA MS/MS was *m/z* 50 - 800. Declustering potential (DP), collision energy (CE), and collision energy spread (CES) were -80 V, -30 eV, and 10 eV, respectively. Instrument control, data acquisition and processing were performed using the PeakView analysis software (AB Sciex, Boston, USA).

Text S3. Possible reasons accounting for the absence of fluorescence detected for BPA, ATP, and BP1

The absence of fluorescence detected by BPA may be related to the isopropyl side chain. Such flexible alkyl chain facilitates the deactivation of excited state BPA via nonradiative pathway (discussed below). The hydroxyl (-OH) and amine (-NH) substituents in ATP molecular structure are important fluorophores. The lack of fluorescence of ATP is possibly due to the fact that bond cleavage occurred rapidly from its lowest lying singlet excited state (S1) (Pozdnyakov et al., 2014). Previous study has reported that UV_{254} irradiation could cause the amide bond cleavage of ATP followed by the photo-Fries rearrangement (Kawabata et al., 2012). BP1 contains several chromophores including phenyl, phenolic, and carbonyl groups. Therefore, its singlet and triplet excited states may involve different electronic configurations, which are favorable for intersystem crossing (ISC) process through spin-orbit coupling (SOC) (Turro et al., 2010). The rapid ISC

process competes with the fluorescence process, resulting in a very low fluorescence quantum yield ($\Phi_F \approx 0$) of benzophenone derivatives (Boscá and Miranda, 1998). In addition, the lack of fluorescence of BP1 may also be explained by its intramolecular charge transfer which can result in fluorescence quenching (Bhasikuttan et al., 1998).

Text S4. Calculation of steady-state concentration of $NO_2^{\bullet}$

According to the above results, reactive radicals such as $HO^{\bullet}$ and $NO_2^{\bullet}$ play critical roles in the NO_2^--sensitized photolysis of phenolic compounds, including BPA, SAL, and BP1. Assuming that the degradation of phenolic compounds is contributed by both direct and indirect photolysis (mediated mainly by $HO^{\bullet}$ and $NO_2^{\bullet}$), the reaction rate constant ($k_{NO2\bullet}$) contributed by $NO_2^{\bullet}$ can be described by the following equation:

$$k_{NO_2\cdot} = k_{obs} - k_{dp} - k_{HO\cdot} \quad \text{(S1)}$$

where k_{obs} is the observed rate constant of sensitized photolysis of phenolic compounds; k_{dp} is the direct photolysis rate constant, which can be calculated by equation (2); $k_{HO\bullet}$ is the reaction rate constant contributed by $HO^{\bullet}$, which can be calculated by $k_{HO\bullet} = k_{HO\bullet,PC}[HO^{\bullet}]_{SS}$. $k_{HO\bullet,PC}$ is the second-order rate constant for the reaction of $HO^{\bullet}$ with phenolic compounds (obtained from literatures, see Table 2), and $[HO^{\bullet}]_{SS}$ is the steady-state concentration of $HO^{\bullet}$.

In the UV_{254}/NO_2^- system, $[HO^{\bullet}]_{SS}$ is mainly determined by its formation rate and consumption reaction rate constants (Eq. (S2)) (Li et al., 2021):

$$[HO\cdot]_{ss} = \frac{2.3E_p^0 \varepsilon_{NO_2^-}^{254}[NO_2^-]\Phi_{NO_2^- \to \cdot OH}}{k_0[NO_2^-] + k_{HO\cdot,PC}[PC]} \quad \text{(S2)}$$

where E_p^0 is the irradiance of incident photons; $\varepsilon_{NO_2^-}^{254}$ is the molar absorption coefficient of NO_2^- at 254 nm; $[NO_2^-]$ is the molar concentration of NO_2^-; $\Phi_{NO_2^- \to \cdot OH}$ is the quantum yield of $HO^{\bullet}$ formed by NO_2^- photolysis at 254 nm (see R(2)); k_0 is the second-order rate constant between $HO^{\bullet}$ and NO_2^- (see R(3)); [PC] is the molar concentration of certain phenolic compound.

In the UV_{254}/NO_2^- system, $[NO_2^{\bullet}]_{SS}$ can be calculated by the following equation (for detailed derivation, please refer to our previous study (Li et al., 2021)):

$$[NO_2^{\cdot}]_{ss} = \sqrt{\frac{k_0(k_{-1} + k_2)[HO\cdot]_{ss}[NO_2^-])}{2k_1k_2}} \quad \text{(S3)}$$

where k_1, k_{-1}, and k_2 are the rate constants of forward, reverse, and hydrolysis reactions of N_2O_4, respectively (Minero et al., 2007). Through the kinetic modeling, we can calculate the second-order rate constant for reaction of $NO_2^{\bullet}$ with phenolic compounds ($k_{NO2\bullet,PC} = k_{NO2\bullet}/[NO_2^{\bullet}]_{ss}$), as tabulated in Table 2.

Tables

Table S1. The physicochemical properties of phenolic compounds used in this study.

Phenolic compound	Molecular structure	Formula	Molecular weight	pK_a	Property
Bisphenol A (BPA)	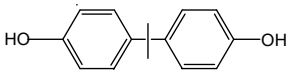	$C_{15}H_{16}O_2$	228	10.29	Plasticizer
Acetaminophen (ATP)	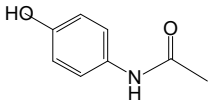	$C_8H_9NO_2$	151	9.86	Analgesic-antipyretic
Salbutamol (SAL)	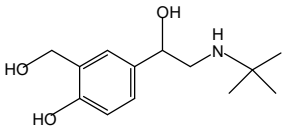	$C_{13}H_{21}NO_3$	239	9.07	Antiasthmatic, β2 adrenoceptor agonis
2, 4-Dihydroxybenzophenone (BP1)	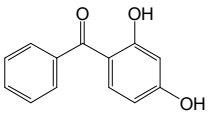	$C_{13}H_{10}O_3$	214	7.22	Sunscreen

Table S2. Characteristics of wastewater water used in this work.

TOC (mg/L)	NO_3^- (mg/L)	NO_2^- (mg/L)	Abs_{254}	Cl^- (mg/L)	Br^- (mg/L)	Na^+ (mg/L)	Mg^{2+} (mg/L)	pH
27	5.348	ND	0.3977	233.590	64	16.033	10.315	8.33

ND: not detected with limit of detection (LOD) 0.016 mg/L

Table S3. Detailed HPLC analytical parameters for measuring compounds in this study[a]

Compound	Molecular structure	Mobile phase composition[b]	Retention time (min)	Detection wavelength (nm)[c]
Bisphenol A (BPA)	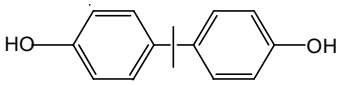	30% H_2O+ 70% MeOH	5.26	275
Acetaminophen (ATP)	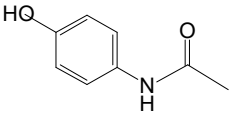	75% H_2O+ 25% MeOH	5.14	243
Salbutamol (SAL)	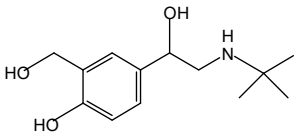	85% H_2O+ 15% MeOH	6.10	271
2, 4-Dihydroxybenzophenone (BP1)	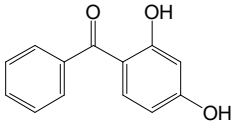	30% H_2O+ 70% MeOH	8.20	271

[a] An Agilent Zorbax Eclipse C18 column (5 μm, 125 mm × 4.6 mm i.d.) was employed for analysis. [b] Isocratic mobile phase was at a flow rate of 1.0 mL min^{-1}. [c] The detection wavelength was chosen according to the maximum absorbance in UV-vis spectrum of individual compound.

Table S4. Mass spectrum data and proposed molecular structures for the intermediate products generated in NO_2^- sensitized photolysis of BPA in aqueous solution.

TPs	RT(time)	Measured exact mass [M-H]$^-$	Theoretical exact mass [M-H]$^-$	Δppm	Formula of derived molecule	MS/MS fragments	Proposed structure
BPA	7.04	227.1084	227.1078	2.9	C15H16O2	227.110、211.0792、133.0674、117.0358、93.0364	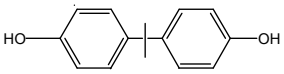
B-1	6.60	243.1028	243.1027	0.6	C15H16O3	243.1060、228.0823、227.0744、149.0625、133.0306、109.0310、93.0360	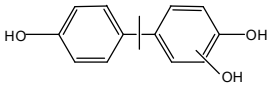
B-2	5.72	259.0978	259.0976	0.9	C15H16O4	259.1033、215.1102、199.0787、198.0706、184.0538	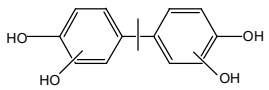
B-3	7.06	256.0981	256.0979	0.8	C15H15O3N		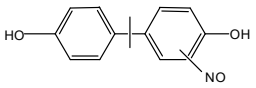
B-4	7.71	272.0932	272.0928	1.4	C15H15O4N	272.0958、257.0722、256.0646、240.0694、227.0738、210.0708、182.0755、167.0522	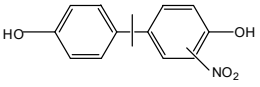
B-5	7.58	288.0875	288.0878	-0.8	C15H15O5N	244.1000、226.0901、211.0667、	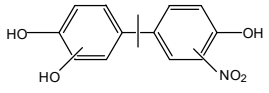

B-6	8.06	317.0781	317.0779	0.7	C15H14O6N2	195.0704、178.0532、108.0237、65.0425、317.0829、285.0561、255.0568、227.0620、212.0376	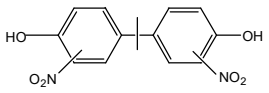
B-7	6.18	304.0829	304.0827	0.7	C15H15O6N	260.0973、228.0722、172.0571	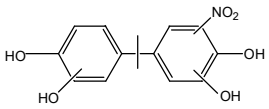
B-8	7.11	333.0728	333.0728	-0.1	C15H14O7N2	333.0768、272.0597	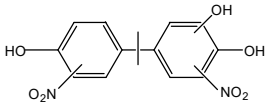
B-9	4.91	138.0209	138.0197	8.9	C6H5O3N	138.0232、108.0250、92.0297	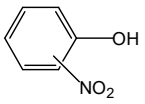
B-10	4.16	154.0153	154.0146	4.8	C6H5O4N	154.0169、124.0179、123.0105、95.0169	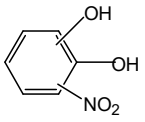
B-11	10.33	151.0774	151.0765	6.5	C9H12O2		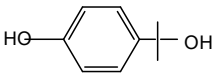
B-12	3.92	167.0719	167.0714	3.4	C9H12O3	149.0591	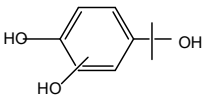
B-13	5.91	196.0622	196.0615	3.5	C9H11O4N	196.0648、178.0544、148.0554	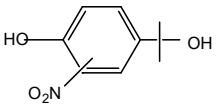
B-14	6.24	212.0564	212.0565	-0.1	C9H11O5N	212.0620、180.0332、137.0148	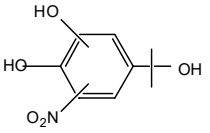

Table S5. Mass spectrum data and proposed molecular structures for the intermediate products generated in NO_2^- sensitized photolysis of ATP in aqueous solution.

TPs	RT(time)	Measured exact mass $[M-H]^-$	Theoretical exact mass $[M-H]^-$	Δppm	Formula of derived molecule	MS/MS fragments	Proposed structure
ATP	3.35	150.0569	150.0561	5.4	C8H9O2N	150.0569、134.0277、118.0300、107.0383	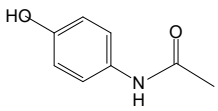
A-1	0.5	150.0570	150.0561	4.8	C8H9O2N	150.0556、118.0330、107.0382	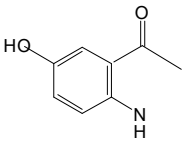
A-2	0.48	166.0515	166.0510	0.4	C8H9O3N		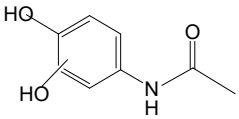
A-3	0.47	182.0463	182.0459	2.3	C8H9O4N	122.0406	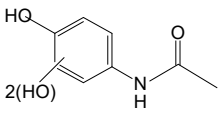
A-4	4.06	179.0463	179.0462	0.4	C8H8O3N2		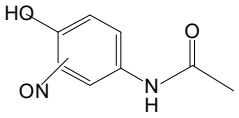
A-5	4.86	195.0419	195.0411	4	C8H8O4N2	195.0440、179.0406、163.0176、152.0247、150.0217、133.0187、122.0264、94.0323	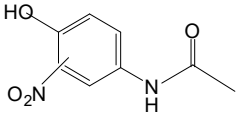
A-6	4.71	211.0363	211.0361	1.2	C8H8O5N2		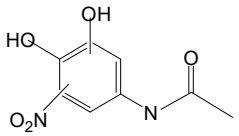
A-7	5.95	240.0266	240.0262	1.5	C8H7O6N3		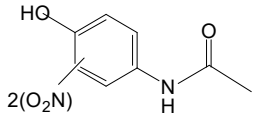

A-8	3.34	108.0452	108.0455	-2.5	C6H7ON		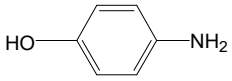
A-9	5.03	138.0207	138.0197	7.2	C6H5O3N	138.0197、108.0236	
A-10	4.3	154.0152	154.0146	3.8	C6H5O4N	123.0116	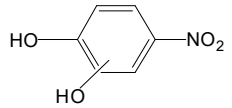
A-11	5.4	183.0055	183.0047	4.6	C6H4O5N2		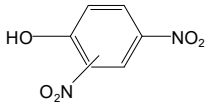
A-12	5.93	198.9994	198.9997	-1.4	C6H4O6N2		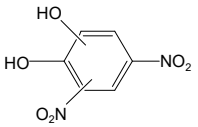
A-13	4.41	299.1029	299.1037	-2.7	C16H16O4N2	299.1060、239.0845	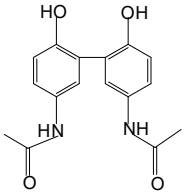
A-14	4.71	315.0989	315.0987	-0.7	C16H16O5N2	178.9602、112.9877	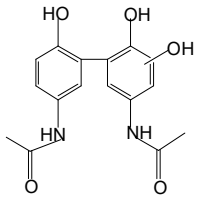
A-15	5.06	331.0939	331.0936	0.9	C16H16O6N2	287.1081、269.0970、226.0904、185.0735、158.0622	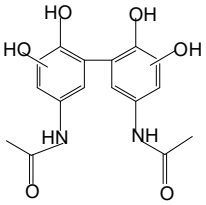
A-16	5.04	328.0908	328.0939	-9.4	C16H15O5N3		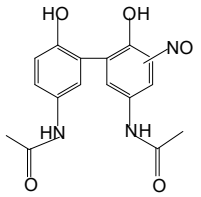
A-17	5.23	344.0884	344.0888	-1.1	C16H15O6N3		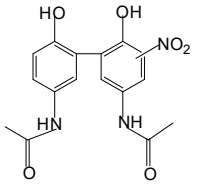
A-18	5.3	360.0826	360.0837	-3.1	C16H15O7N3		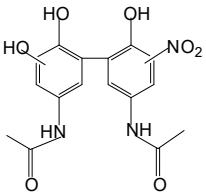

A-19	5.3	376.0783	376.0796	-1	C16H15O8N3	376.0891、332.0964、297.0809	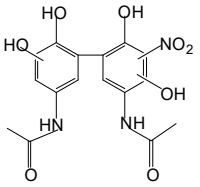

Table S6. Mass spectrum data and proposed molecular structures for the intermediate products generated in NO_2^- sensitized photolysis of SAL in aqueous solution.

TPs	RT(time)	Measured exact mass [M-H]$^-$	Theoretical exact mass [M-H]$^-$	Δppm	Formula of derived molecule	MS/MS fragments	Proposed structure
SAL	3.63	238.1454	238.1449	2.3	C13H21O3N	220.1368、218.1210、190.1257、163.0653、160.0394	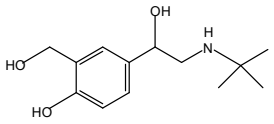
S-1	8.08	270.1347	270.1347	0	C13H21O5N		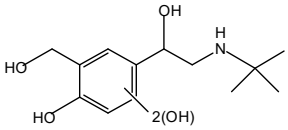
S-2	4.17	283.1302	283.1300	1	C13H20O5N2	283.1325、263.1074、235.1118、208.0505、151.0286	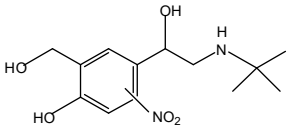
S-3	0.48	299.1254	299.1249	2	C13H20O5N2		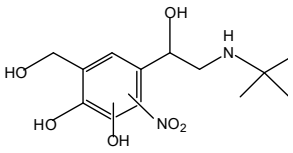
S-4	3.91	267.1352	266.1272	0.8	C13H20O4N2	181.0463、138.0533、123.0324、110.9450	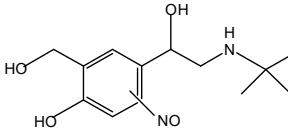
S-5	0.57	153.0570	153.0557	8.4	C8H10O3		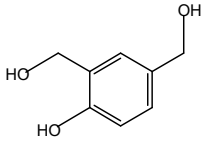
S-6	3.92	151.0409	151.0401	5.8	C8H8O3	149.0240、121.0311、92.0295	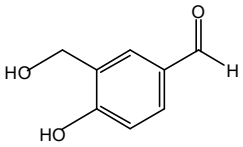

Table S7. Mass spectrum data and proposed molecular structures for the intermediate products generated in NO_2^- sensitized photolysis of BP1 in aqueous solution.

TPs	RT(time)	Measured exact mass $[M-H]^-$	Theoretical exact mass $[M-H]^-$	Δppm	Formula of derived molecule	MS/MS fragments	Proposed structure
BP1	7.22	213.0559	213.0557	0.7	C13H10O3	213.0579、169.0673、143.0518、135.0100、91.0208、65.0060	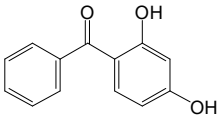
P-1	6.55	229.0508	229.0506	0.8	C13H10O4		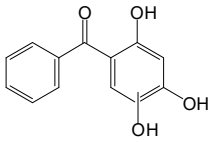
P-2	5.62	245.0434	245.0455	-8.6	C13H10O5	133.0664、77.0414	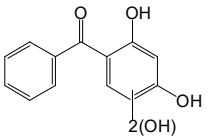
P-3	7.71	258.0408	258.0408	0	C13H9O5N	258.0448、241.0404、224.0365、211.0421、167.0515	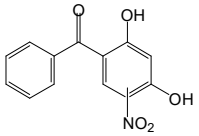
P-4	7.36	274.0351	274.0357	-2.4	C13H9O6N	274.0393、154.0149、137.0118、93.0344	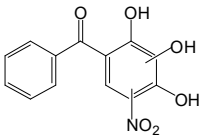
P-5	6.5	242.0460	242.0459	0.6	C13H9O4N	242.0491、225.0459、211.0424、181.0556、145.0310、120.0105	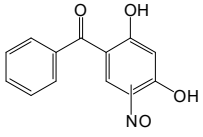
P-6	5.56	121.0306	121.0295	9.2	C7H6O2	121.0372、77.0418	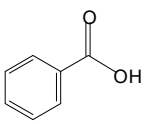

P-7	6.72	109.0304	109.0295	8.5	C6H6O2	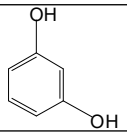

Table S8. Calculation of the screening factor S_λ for SRNOM[a].

SRNOM（mg/L）	S_λ (BPA+NO_2^-)	S_λ (ATP+NO_2^-)	S_λ (SAL+NO_2^-)	Sλ (BP1+NO_2^-)
1	0.9371	0.9414	0.9377	0.9418
2	0.8897	0.8958	0.8886	0.8968
5	0.7689	0.7812	0.7684	0.7830

[a] The reaction solution contains 10 μM individual phenolic compounds, 100 μM NO_2^- with different concentrations of SRNOM.

Figures.

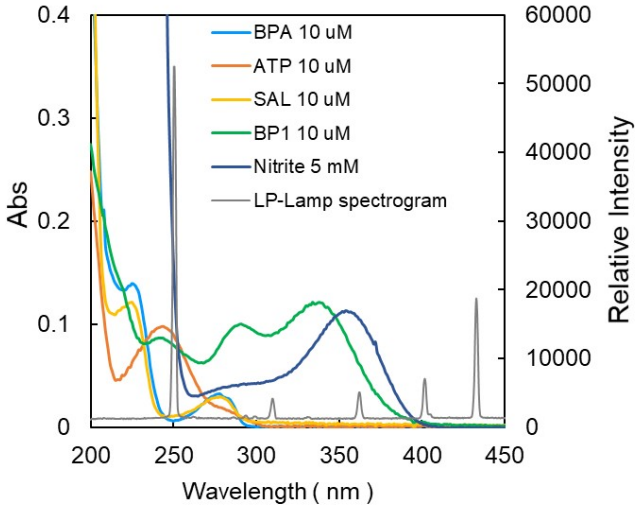

Fig. S1. UV-Vis absorption spectra of aqueous solutions of BPA, ATP, SAL, BP1 and NO_2^-. The emission spectrum of the LP-Hg lamp is also shown in the figure.

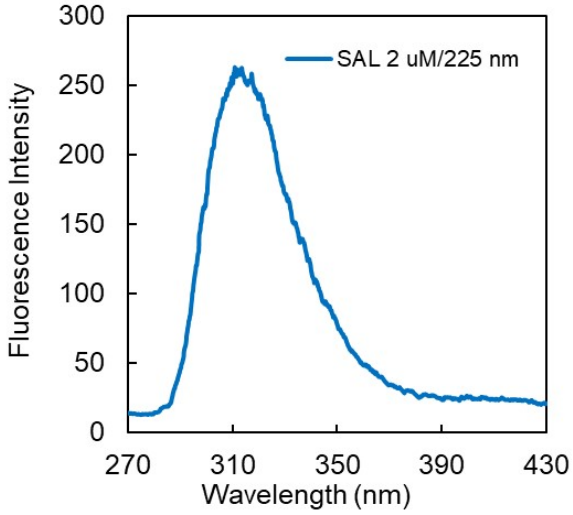

Fig. S2. Fluorescence spectra of the aqueous solutions of SAL. The concentration of SAL was 2 μM and the excitation wavelength was 225 nm.

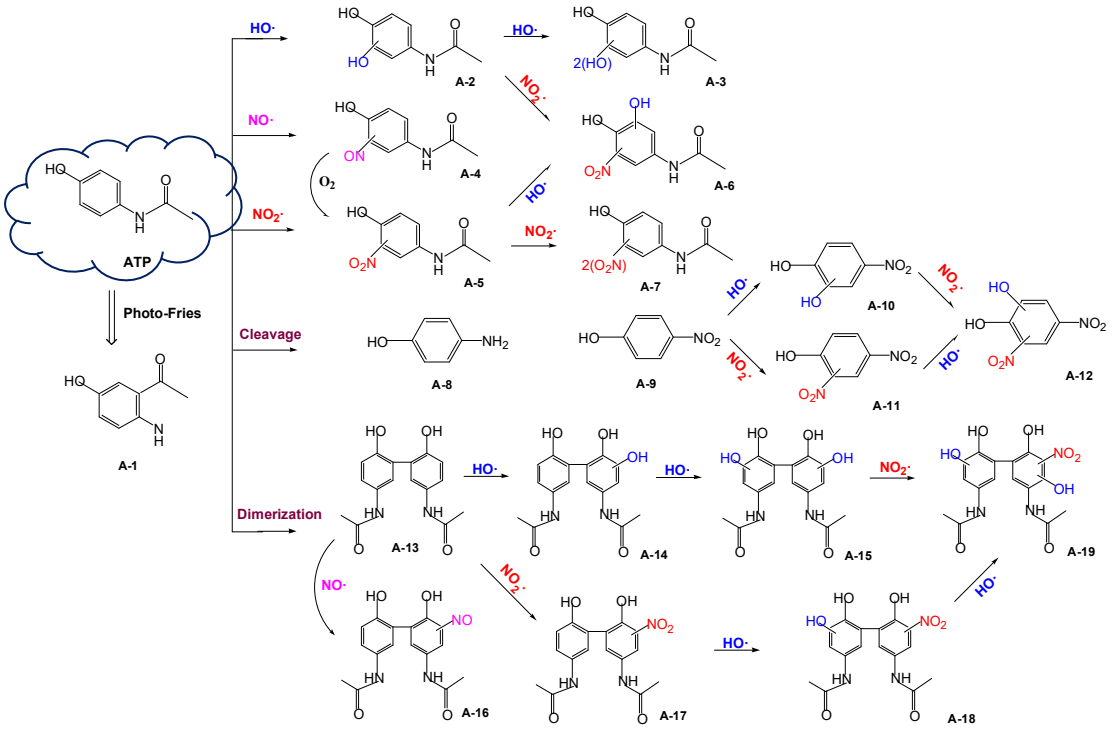

Fig. S3. Transformation pathways for the NO_2^--sensitized photolysis of ATP in aqueous solution under UV_{254} irradiation. Note that there may be different isomers of the dimer which are not shown in this figure.

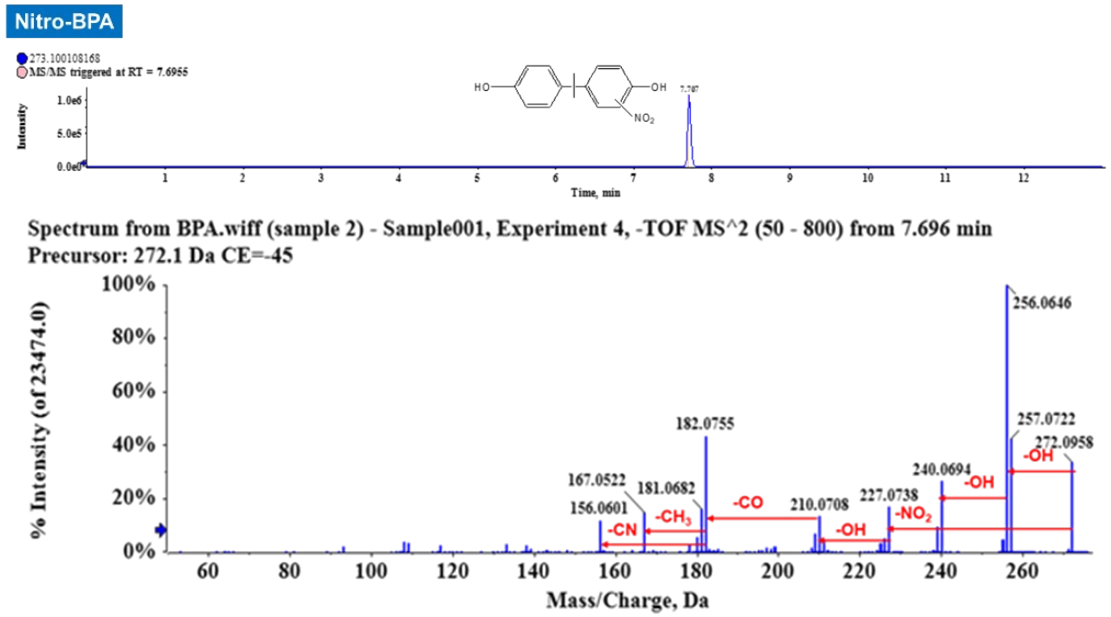

Fig. S4. Extracted ion chromatograph of the nitrated product of BPA (upper panel), and MS/MS spectrum of the nitrated product of BPA (down panel).

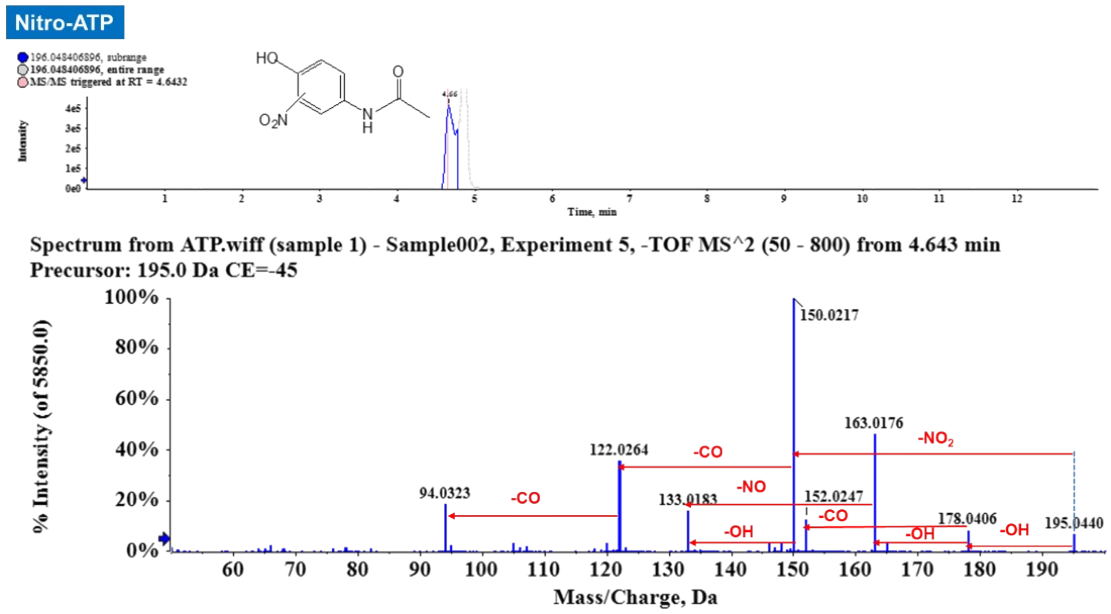

Fig. S5. Extracted ion chromatograph of the nitrated product of ATP (upper panel), and MS/MS spectrum of the nitrated product of ATP (down panel).

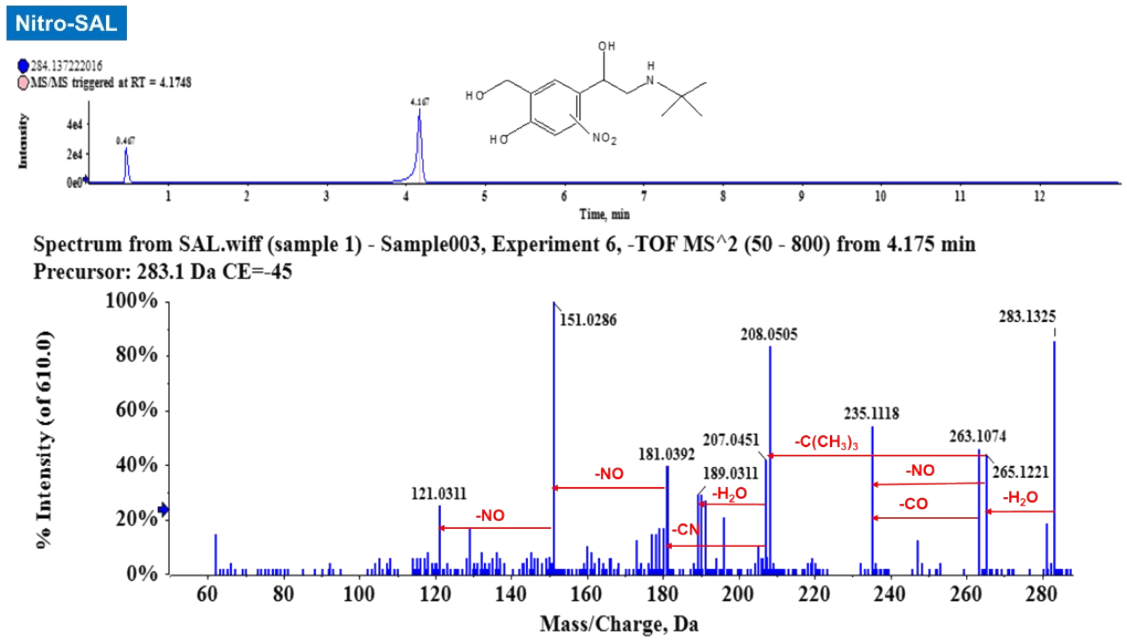

Fig. S6. Extracted ion chromatograph of the nitrated product of SAL (upper panel), and MS/MS spectrum of the nitrated product of SAL (down panel).

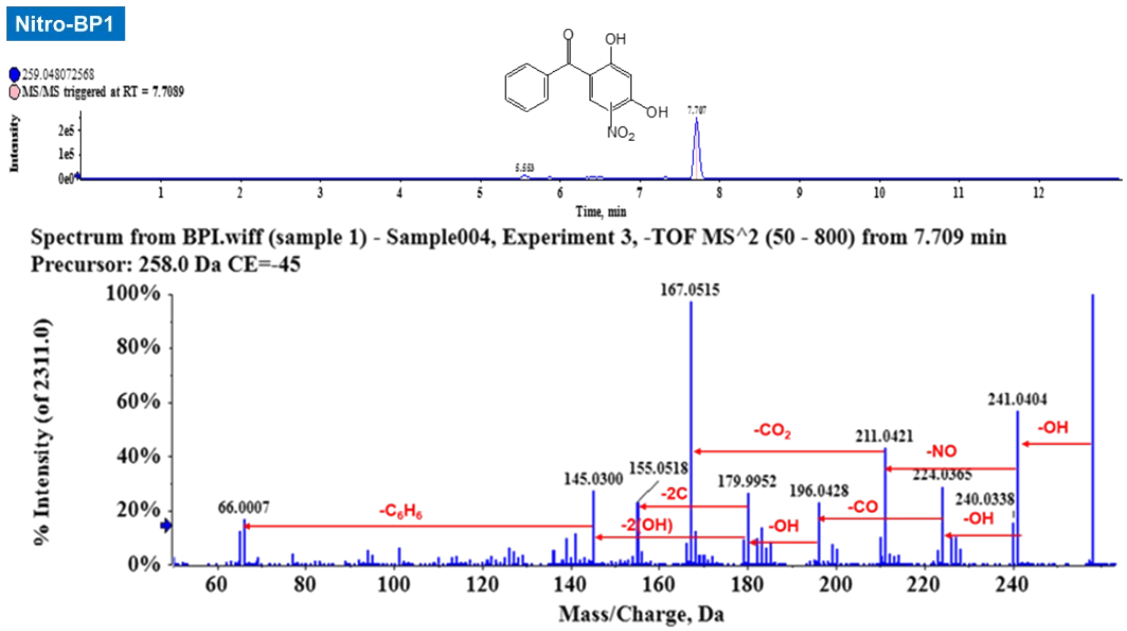

Fig. S7. Extracted ion chromatograph of the nitrated product of BP1 (upper panel), and MS/MS spectrum of the nitrated product of BP1 (down panel).

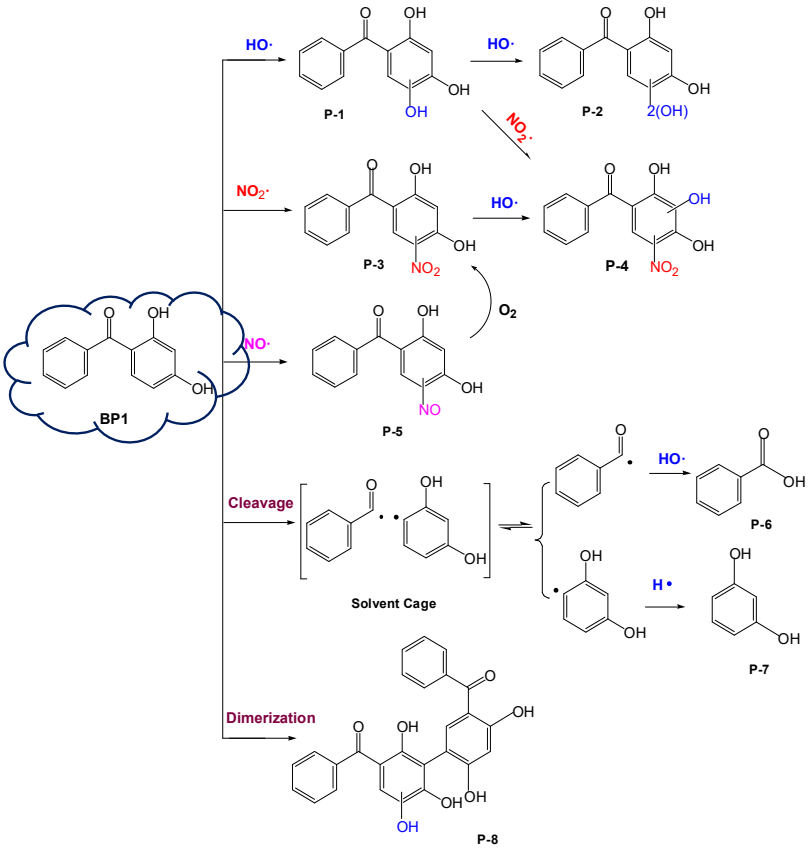

Fig. S8. Transformation pathways for the NO_2^- sensitized photolysis of BP1 in aqueous solution under UV_{254} irradiation.

References

Bhasikuttan, A. C., Singh, A.K., Palit, D.K., Sapre, A.V., Mittal, J.P., 1998. Laser flash photolysis studies on the monohydroxy derivatives of benzophenone. J. Phys. Chem. A. 102, 3470-3480.

Boscá, F., Miranda, M. A., 1998. New Trends in Photobiology (Invited Review) Photosensitizing drugs containing the benzophenone chromophore. J. Photochem. Photobiol. B: Biol. 43(1), 1-26.

Kawabata, K., Sugihara, K., Sanoh, S., Kitamura, S., Ohta, S., 2012. Ultraviolet-photoproduct of acetaminophen: Structure determination and evaluation of ecotoxicological effect. J. Photochem. Photobiol. A: Chem. 249, 29-35.

Li, Y., Qin, H., Li, Y., Lu., Zhou, L., Chovelon, J.M., Ji, Y., 2021. Trace level nitrite sensitized photolysis of antimicrobial agents parachlormetaxylenol and chlorophene in water. Water Res. 200, 117275.

Minero, C., Chiron, S., Falletti, G., Maurino, V., Pelizzetti, E., Ajassa, R., Carlotti, M.E., Vione, D., 2007. Photochemical processes involving nitrite in surface water samples. Aquat. Sci. 69, 71-85.

Pozdnyakov, I.P., Zhang, X., Maksimova, T.A., Yanshole, V.V., Wu, F., Grivin, V.P., Plyusnin, V.F., 2014. Wavelength-dependent photochemistry of acetaminophen in aqueous solutions. J. Photochem. Photobiol. A: Chem. 274, 117-123.

Turro, N.J., Ramamurthy, V., Scaiano, J.C., 2010. Modern Molecular Photochemistry of Organic Molecules. University Science Books.